

actions. This competition is reflected by the low yield of  $\text{NA}^-$  measurable (as given by the low-oxidation efficiency). Again, the calculated rate constants for adduct formation increase with increasing nitro compound redox potential ( $\text{NB} < \text{PNAP} < \text{NF}$ ).

The  $\alpha$ -hydroxy radicals, formed by H abstraction, dissociate to form  $\text{R}^-$  at the  $\text{p}K_a \sim 10$ .<sup>16</sup> The same species  $\text{R}^-$  generated in alkaline solution by  $e_{\text{aq}}^-$  attachment to R have previously been shown to undergo rapid electron-transfer oxidation to restore R, and the rate constants are similar to those shown in Table I.<sup>17</sup>

(16) K. D. Asmus, A. Henglein, A. Wigger, and G. Beck, *Ber. Bunsenges. Phys. Chem.*, **70**, 756 (1966).

(17) G. E. Adams, B. D. Michael, and R. L. Willson, *Advan. Chem. Ser.*, No. **81**, 289 (1968).

The  $\text{RH}^+$  species formed by electron-transfer oxidation of  $\cdot\text{RH}$ , at neutral pH, will also rapidly dissociate to give a stable molecule R. For crotyl and allyl alcohols, deprotonation of  $\cdot\text{ROH}$  and  $\text{ROH}^+$  does not produce a stable species, and this may, in part, explain the low-oxidation efficiencies observed. Such specificities for reactions of biochemical free radicals with nitroaromatic compounds and other electron-affinic agents are now being studied by pulse radiolysis in an effort to explain the relative biological efficiencies of different cellular radiosensitizers.

**Acknowledgments.** We thank our colleagues of the Research Chemistry and Medical Biophysics Branches for helpful discussions.

## Electron Paramagnetic Resonance Studies of Equilibrium and Kinetics of Solvation and Ion Pair Structure. Solvation of Fluorenone Ketyls by Alcohol

Kazuo Nakamura, B. F. Wong, and Noboru Hirota\*

Contribution from the Department of Chemistry, State University of New York at Stony Brook, Stony Brook, New York 11790.

Received June 14, 1972

**Abstract:** Solvation of alkali metal ketyls of fluorenone by various alcohols was investigated. The effects of solvation on the alkali metal splittings and carbonyl  $^{13}\text{C}$  splittings were carefully investigated. The observed changes of splittings were explained in terms of the solvation processes involving three solvated species. The possible structures of the solvated ion pairs were suggested from the values of splittings to best fit the experimental values. The line broadening due to the modulation of isotropic hyperfine splittings by solvation processes was investigated in several systems. The rates of formation of the solvated complexes and the lifetimes of the solvated complexes are estimated in sodium fluorenone in *i*-PrOH-THF mixtures.

Radical ions prepared by the alkali metal reduction of aromatic molecules form ion pairs in various organic solvents.<sup>1</sup> Since the structures and reactivities of ion pairs are strongly affected by solvation processes,<sup>2-4</sup> it is desirable to know the details of the solvation processes in order to understand the behavior of ion pairs in a variety of solutions. Epr is suited to investigating the microscopic details of the solvation processes, but most of the previous solvation studies of radical anions were limited to the dissociated free ions.<sup>5-10</sup> Furthermore, no data on the rates of formation and dissociation of solvated complexes were obtained in the previous studies. Accordingly,

we have attempted to investigate the process of solvation of both cations and anions. The process of cation solvation by polar solvents such as DMF was described in detail in a previous paper.<sup>4</sup> In the present paper we discuss the solvation of ion paired anions by various alcohols.

Many radical anions are unstable in solutions containing protic solvents such as alcohol. However, we found that many ketyls are stable in the mixtures of alcohol and ether. Ketyls form alcohol solvated complexes through hydrogen bonding to the carbonyl oxygen atom. Since the cation is situated in the neighborhood of the carbonyl oxygen, solvation by alcohol can change the ion pair structure. The structural changes of ion pairs should be reflected in changes of the alkali metal splittings as well as the proton and the carbonyl  $^{13}\text{C}$  splittings.

In this work we chose fluorenone ketyls and investigated the solvation of various alcohols to ion paired fluorenones. The solvation of free fluorenone anion by alcohol in DMF solution was studied previously by Luckhurst and Orgel.<sup>7</sup> Here we attempt to elucidate the detailed steps of the solvation processes and the structures of the solvated ion pairs and to study the kinetics of the solvation and desolvation processes.<sup>11</sup>

(1) For example, see (a) "Ions and Ion Pairs in Organic Reactions," Vol. 1, M. Szwarc, Ed., Wiley, New York, N. Y., 1972; (b) M. Szwarc, *Accounts Chem. Res.*, **2**, 87 (1969).

(2) N. Hirota, R. Carraway, and W. Schook, *J. Amer. Chem. Soc.*, **90**, 3611 (1968).

(3) B. F. Wong and N. Hirota, *J. Amer. Chem. Soc.*, **94**, 4419 (1972).

(4) K. S. Chen, S. W. Mao, K. Nakamura, and N. Hirota, *J. Amer. Chem. Soc.*, **93**, 6004 (1971).

(5) E. W. Stone and A. H. Maki, *J. Chem. Phys.*, **36**, 1944 (1962); *J. Amer. Chem. Soc.*, **87**, 454 (1965).

(6) J. Gendell, J. H. Freed, and G. K. Fraenkel, *J. Chem. Phys.*, **37**, 2832 (1962).

(7) G. R. Luckhurst and L. E. Orgel, *Mol. Phys.*, **8**, 117 (1964).

(8) P. Ludwig, T. Layloff, and R. N. Adams, *J. Amer. Chem. Soc.*, **86**, 4568 (1964).

(9) J. Q. Chambers and R. N. Adams, *Mol. Phys.*, **9**, 413 (1965).

(10) N. T. Hetrich and T. Layloff, *J. Amer. Chem. Soc.*, **91**, 6910 (1969).

(11) Preliminary report of this work was given in a letter: K. Nakamura and N. Hirota, *Chem. Phys. Lett.*, **3**, 137 (1969).

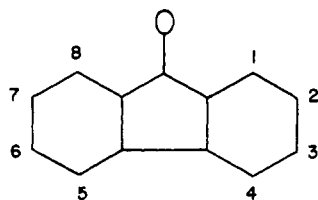


Figure 1. The molecular structure and numbering system of ring protons of fluorenone.

radical increases in the following order: MeOH < EtOH < *n*-PrOH < *n*-BuOH > *i*-PrOH < *t*-BuOH. In *i*-PrOH and *t*-BuOH mixtures, samples are sufficiently stable to allow epr measurements even several days after the addition of alcohol, while in MeOH and EtOH, samples were only stable long enough to make the measurements within several hours after the addition.

Intensities of the epr signals of fluorenone ketyls in the mixtures of alcohol and THF decrease irrevers-

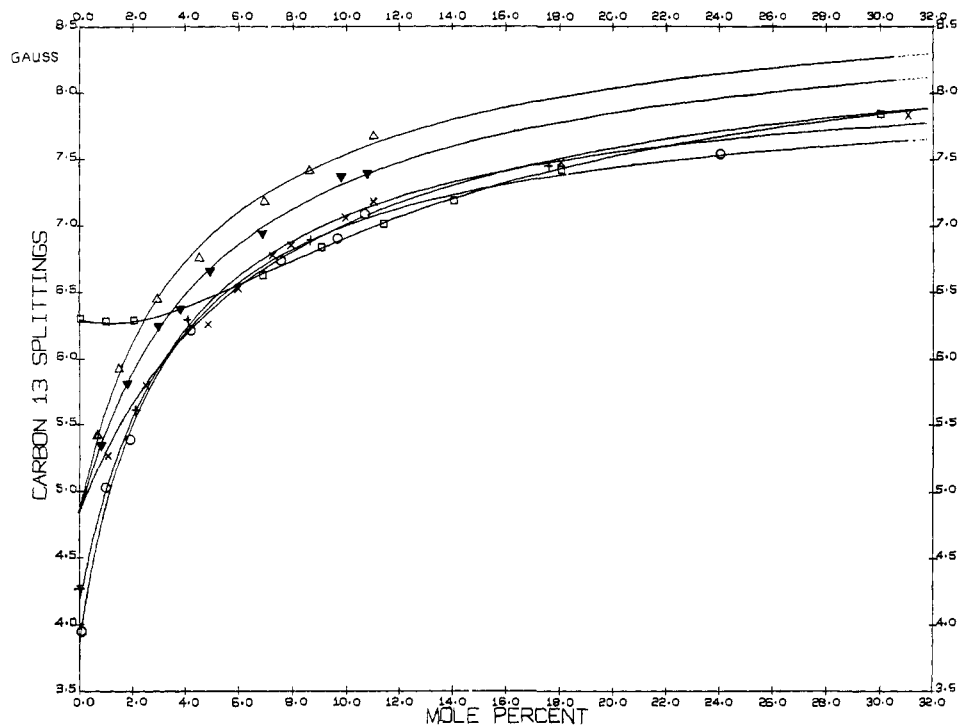


Figure 2. Changes of the  $^{13}\text{C}$  splittings of fluorenone ketyls by the addition of various alcohols. The points indicate the experimental values. The curves give the predicted changes of the splittings obtained by using eq 3 and the values listed in Table I. These curves were drawn by a computer. In all cases THF was used as an ethereal solvent: ( $\square$ ) Li, *i*-PrOH; ( $\Delta$ ) Na, MeOH; ( $\blacktriangledown$ ) Na, EtOH; ( $\times$ ) Na, *i*-PrOH; (+) K, *i*-PrOH; ( $\circ$ ) Cs, *i*-PrOH.

## Experimental Section

Preparation of radicals and epr measurements followed the standard procedures described elsewhere.<sup>12</sup> Ketyls were prepared in the ethereal solvents and then a desired amount of alcohol was added. The sample cell contains a vacuum stop cock and a tapered joint through which a known amount of alcohol was added. Alcohol was dried by refluxing with  $\text{CaH}_2$  for several hours, distilled, and stored in a bottle containing fluorenone ketyls. A small amount of alcohol was transferred into a graded capillary tube through a vacuum line and then transferred into a sample cell. THF was used as the ethereal solvent throughout this work. The radical concentration in solution was estimated to be  $10^{-3}$ – $10^{-4}M$ .

## Results and Discussion

### 1. Stabilities of Radicals in Alcohol Mixtures.

**A. Dependence on the Type of Radicals.** The following radicals decomposed quickly with the addition of alcohol and gave no epr signal: hydrocarbon anions, 2,2'-bipyridyls, and benzonitriles. The following radicals gave epr signals after the addition of alcohol: ketyls, nitrobenzene, and quinoxaline anions.

**B. Stabilities of Fluorenone Ketyls.** Stabilities of radicals in alcohol mixtures depend on the nature of the alcohol and generally do not depend on the alkali metal counterions. For fluorenone ketyls the stability of the

radical is higher in alcohol mixtures than in THF, especially at lower temperatures, indicating that the radical ions are more unstable at lower temperatures. This was particularly notable in MeOH mixtures.

### 2. Effects of Alcohol Addition on the Epr Parameters.

Since fluorenone ketyls are very stable we have used them for the detailed investigations. The molecular structure and the numbering system of fluorenone is given in Figure 1. Ketyls usually exist as ion pairs in the THF-alcohol mixtures up to 50% of alcohol at room temperature, although the epr spectra due to the dissociated ions are observable in the high percentage mixtures of alcohol. At lower temperatures, on the other hand, a larger extent of dissociation was observed. Even at 2% of *i*-PrOH sodium ion pairs are almost completely dissociated at  $-70^\circ$ . In general, a drastic increase of dissociation was observed at lower temperatures.

All hyperfine splittings (hfs) change upon the addition of alcohol, especially the alkali metal splittings,  $^{13}\text{C}$  splittings of carbonyl carbon, and proton splittings at the 2 and 7 positions. A linear relationship between the carbonyl  $^{13}\text{C}$  splitting and the proton splittings at the 2 and 7 positions was noted.

#### A. Changes of the Carbonyl $^{13}\text{C}$ Splittings.

Changes

(12) N. Hirota, *J. Amer. Chem. Soc.*, **89**, 32 (1967).

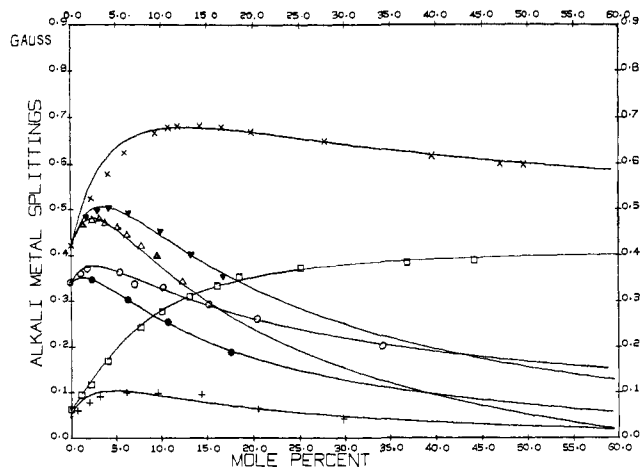
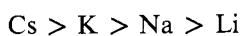


Figure 3. Changes of the alkali metal splittings by the addition of alcohol. The points indicate the experimental values. The curves give the predicted changes obtained by using eq 3 and the values listed in Table I. The curves are drawn by a computer: ( $\square$ ) Li, PrOH; ( $\Delta$ ) Na, MeOH; ( $\blacktriangledown$ ) Na, EtOH; ( $\times$ ) Na, *i*-PrOH; (+) K, *i*-PrOH; (O) Cs, *i*-PrOH.

in the  $^{13}\text{C}$  splittings are given in Figure 2. Characteristic general trends are summarized in the following.

i. The increase of the  $^{13}\text{C}$  splittings and therefore the extent of solvation depends on the solvent and counterion. The ease of solvation increases in the following order



ii. The asymptotic values of the  $^{13}\text{C}$  splittings depend only slightly on the nature of the cation. The effect of solvation on the spin distribution seems to be more than the effect of ion pair formation at large fractions of alcohol.

**B. Changes of Alkali Metal Splittings.** The changes of the alkali metal splittings with the addition of alcohol at room temperature are shown in Figure 3. The following are the general trends.

i. The alkali-metal splittings increase with the addition of alcohol in the region of low concentration of alcohol but reach a maxima and then decrease, indicating that more than one solvation step is involved. The positions of the maxima and the amount of decrease strongly depend on the individual system.

ii. For the same cation the increase of the metal splitting with the addition of alcohol is in the following order: *i*-PrOH > EtOH > MeOH.

iii. For a given alcohol the relative increase of the splitting is in the following order: Li > Na > K > Cs. The alkali metal splittings of the ketyls with large cations do not increase much with the addition of alcohol.

iv. The decrease of the splitting in the region of a large fraction of alcohol for a given cation but a different alcohol is in the order MeOH > EtOH > *i*-PrOH and for a given alcohol but a different alkali metal ion Cs > K > Na > Li.

**C. Temperature Dependence of  $^{13}\text{C}$ , Proton, and Alkali Metal Splittings.** Changes of the alkali metal splittings at different temperatures were studied in detail in the case of Na-*i*-PrOH-THF. The changes of the proton splittings were also studied in the same

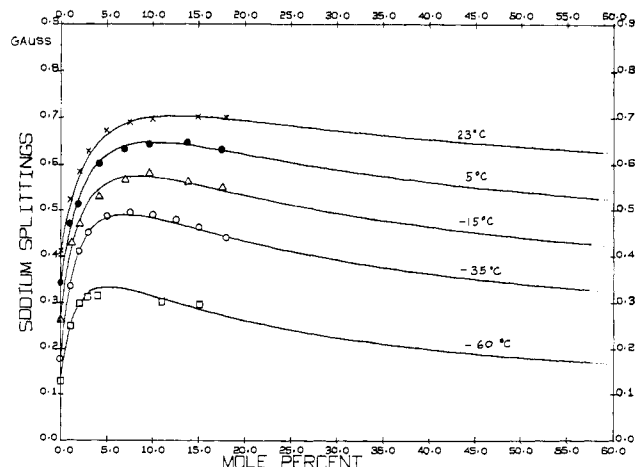


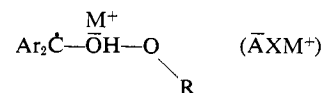
Figure 4. Changes of the sodium splittings by the addition of *i*-PrOH at different temperatures. The points are experimental values. Curves are obtained by using eq 3 and the values listed in Table I: ( $\times$ ) 23°, ( $\blacktriangledown$ ) 5°, ( $\Delta$ ) -15°, (O) -35°, ( $\square$ ) -60°.

system at different temperatures. In Figure 4 changes of sodium splittings at different temperatures are shown. It is shown that the decrease of the sodium splittings at a large fraction of alcohol becomes more pronounced at low temperatures.

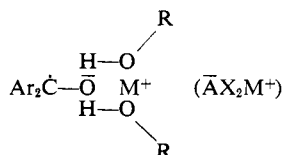
**D. Correlations between the Changes in the  $^{13}\text{C}$  and the Alkali Metal Splittings.** If the solvation processes responsible for the changes in the  $^{13}\text{C}$  and the proton splittings are the same as those responsible for the changes of the alkali metal splittings, there should be a one-to-one correspondence between these changes. While this appears to be the case in certain systems, this is not generally clear from the data shown in these figures. This correspondence, however, will be fully confirmed by the detailed analysis given in section 3.

**3. The Model of Solvated Species and the Solvation Schemes.** Although in many systems the initial increases of the  $^{13}\text{C}$  splittings can be explained by the formation of a 1:1 solvated complex, the complete explanation of the changes in several systems requires the inclusion of the formation of a 1:2 solvated complex as the fraction of alcohol increases. The decrease of the alkali metal splittings at the large fraction of alcohol also indicates the second solvated complexes. The slight decrease of the  $^{13}\text{C}$  splitting in the Li ketyl at the initial stage of the addition of alcohol indicates that in the case of Li a solvated complex with weaker electrostatic interaction is formed at first. It is known from our previous studies that the solvation of cation by polar solvent decreases the electrostatic interaction.<sup>4</sup> Therefore, the initial solvated complex in the case of lithium is likely to involve the solvation of the cation by alcohol. Based on these observations we postulate the formation of the following three solvated species as the major species.

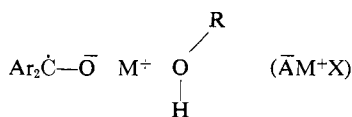
i. Solvation of the anion by one alcohol and the increase of the  $^{13}\text{C}$  and alkali metal splitting.



ii. Solvation of the anion by two alcohols, further increase of the  $^{13}\text{C}$  splitting, and the decrease of the alkali metal splitting.



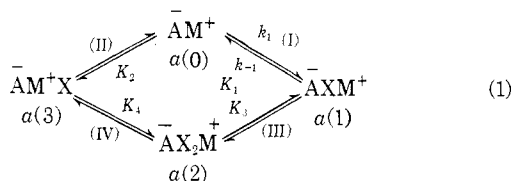
iii. Solvation of the cation by an alcohol and the decrease of the  $^{13}\text{C}$  splitting.



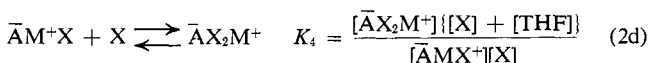
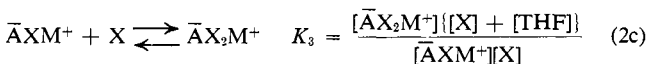
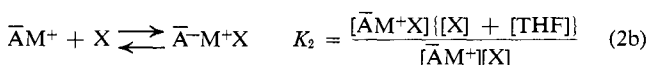
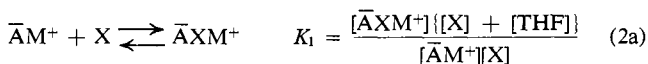
It is possible to consider the other solvated species such as  $\overline{\text{A}}\text{XM}^+\text{X}$  (one alcohol solvates the cation and another solvates the anion) or  $\overline{\text{A}}\text{M}^+\text{X}_2$  (two alcohols solvate the cation). However, these are considered to be negligible based on the observed changes of the splittings.

If the suggested model of solvation is appropriate, we should be able to explain all the observed changes in the  $^{13}\text{C}$ , proton, and alkali metal splittings consistently by assigning reasonable values of the splitting constants to each solvated complex and assuming appropriate equilibrium constant.

The most general solvation scheme including the above complex can be written as



Here  $a(0)$ ,  $a(1)$ ,  $a(2)$ , and  $a(3)$  are the splittings for the unsolvated and solvated ketyls.  $K$ 's are the equilibrium constants and are defined as follows.



Here X represents the alcohol. The equilibrium constants are defined by the above equations for the sake of convenience in expressing the changes of the splittings as the functions of mole per cent of alcohol. Strictly speaking activities should be used instead of concentrations in expressing equilibria. However, the activities are not known and we use concentrations throughout this paper. The observed hyperfine splittings are given by

$$a = \frac{a(0) + \{a(1)K_1 + a(2)K_2\}\chi + a(3)K_1K_3\chi^2}{1 + (K_1 + K_2)\chi + K_1K_3\chi^2} \quad (3)$$

where  $\chi$  is the mole fraction of alcohol. For most systems, except the case of lithium, process II can be neglected compared with process I. When the fraction of alcohol is small, the second-order term is neg-

ligible. In this limiting case eq 3 is reduced to the well-known simple formula<sup>1</sup>

$$a = \frac{a(0) + a(1)K_1\chi}{1 + K_1\chi}$$

This equation accounts reasonably well for the initial changes of the  $^{13}\text{C}$  splittings in most systems.  $K_1$  can be estimated from this equation.

Using eq 3 we have made computer fits of the splittings vs.  $\chi$  curves. These are shown as the curves in Figure 2-4. Quite clearly both  $^{13}\text{C}$  and alkali metal splittings are fitted consistently with the same equilibrium constants, strongly suggesting that the solvation processes responsible for the change of the  $^{13}\text{C}$  splittings and the alkali metal splittings are the same.

Although the experimental results were reproduced well by eq 3, the appropriateness of the assigned values of the splittings has to be checked very carefully in view of the corresponding solvation structures. The justification and the interpretation of the assigned values are given in the following discussions.

**4. Structures of the Solvated Ion Pairs and the Choices of the Assigned Splittings.** **A. The Structure of  $\overline{\text{A}}\text{XM}^+$  and the Alkali Metal and  $^{13}\text{C}$  Splittings ( $a_c$ ).** The question of the position of the cation in the ketyl ion pairs was discussed in detail in the previous paper.<sup>4</sup> It is believed that the cation moves from an "in the plane" position A to an "above the plane" position B as temperature increases, although the exact nature of this motion is not yet completely clear in most systems (Figure 5). In ketyls with smaller cations, the "in the plane" position is favored, but in the ketyls with larger cations, position B is more favored. The metal ion is solvated by the ethereal solvents, and the anion solvation by the alcohol may affect the structure of the solvation sphere of the cation. Therefore, the way the ion pair structure is affected by the alcohol solvation may be rather complex. Nevertheless, the observed trends in the changes of the splittings by the formation of the first solvated complex seem to be well rationalized by the following simple model.

If the most favorable position for both alcohol solvation and cation association is the "in the plane position," A, the alcohol competes with the cation for solvation at this position. Then the probability of finding the cation in the B position increases greatly with the solvation of the alcohol. On the other hand, if the most favorable position for the cation is already the "above the plane position," B, the alcohol solvation has little effect on the structure of the ion pair. When the alcohol is more bulky the ion pair structure is expected to be affected more by solvation. These predictions are well borne out by the observations given in Figure 3. The larger the size of the alcohol, the larger the changes in the metal splittings. The relative change of the splitting is the largest for the lithium ion pair where the ion pair structure is close to the A form at room temperature but the least for the Cs ketyl where the structure is already close to the B form. In the case of sodium the ion pair changes from A to B as the temperature is raised.<sup>4</sup> At a higher temperature (100° or higher) the ion pair structure is considered to be close to B. Alcohol solvation causes very small changes in  $a_{\text{Na}}$  at these temperatures, supporting this

Table I. Values Used for Obtaining the Curves Given in Figures 1-4

(A)													
System	Temp, °C	<sup>13</sup> C splittings, G				Alkali metal splittings, G				Equilibrium constants			
		<i>a<sub>C</sub></i> (0)	<i>a<sub>C</sub></i> (1)	<i>a<sub>C</sub></i> (2)	<i>a<sub>C</sub></i> (3)	<i>a<sub>M</sub></i> (0)	<i>a<sub>M</sub></i> (1)	<i>a<sub>M</sub></i> (2)	<i>a<sub>M</sub></i> (3)	<i>K</i> <sub>1</sub>	<i>K</i> <sub>2</sub>	<i>K</i> <sub>3</sub>	<i>K</i> <sub>4</sub> '
Li, <i>i</i> -PrOH	24	6.30	7.90	4.50	9.50	0.06	0.42	0.35	0.20	3.0	6.0	Small	15.0
Na, MeOH	24	4.85	7.90	4.50	9.00	0.41	0.65	0.55	-0.22	33.0	3.0	5.0	Small
Na, EtOH	24	4.85	7.85	4.50	8.80	0.41	0.75	0.55	-0.07	22.0	2.5	6.0	Small
Na, <i>i</i> -PrOH	24	4.85	7.80	4.50	8.70	0.41	0.92	0.60	0.46	18.0	2.0	4.0	Small
K, <i>i</i> -PrOH	24	4.20	7.70	4.00	8.30	0.05	0.18	0.10	-0.03	30.0	3.0	6.0	Small
Cs, EtOH	24	3.90				0.34	0.41	0.35	-0.06	30.0	0.1	5.5	Small
Cs, PrOH	24	3.90	7.30	3.70	8.20	0.34	0.45	0.35	0.02	40.0	0.1	4.0	Small

(B)													
System	Temp, °C	Proton splittings, G				Sodium splittings, G				Equilibrium constants			
		<i>a<sub>H</sub></i> (0)	<i>a<sub>H</sub></i> (1)	<i>a<sub>H</sub></i> (2)	<i>a<sub>H</sub></i> (3)	<i>a<sub>Na</sub></i> (0)	<i>a<sub>Na</sub></i> (1)	<i>a<sub>Na</sub></i> (2)	<i>a<sub>Na</sub></i> (3)	<i>K</i> <sub>1</sub>	<i>K</i> <sub>2</sub>	<i>K</i> <sub>3</sub>	
Na, <i>i</i> -PrOH	5	0.16	0.34	0.10	0.33	0.34	0.87	0.58	0.39	28	2.0	4.0	
Na, <i>i</i> -PrOH	-15					0.26	0.78	0.54	0.28	37	2.0	4.0	
Na, <i>i</i> -PrOH	-35	0.115	0.32	0.10	0.38	0.18	0.70	0.50	0.20	42	2.0	5.0	
Na, <i>i</i> -PrOH	-60					0.13	0.50	0.40	0.07	45	2.0	6.0	

model. These situations are schematically shown in Figure 5.

The <sup>13</sup>C splittings (*a<sub>C</sub>*) of the solvated complexes should be much larger than those for unsolvated ion pairs. Since the limiting values of *a<sub>C</sub>* in the high-concentration region of alcohol represent those of 1:2 solvated complexes, the estimated values of *a<sub>C</sub>* have large uncertainties. However, they were estimated to be 7-8 G. The difference in <sup>13</sup>C splittings between the solvated and unsolvated ion pairs gives the strength of the perturbation due to the alcohol solvation in each pair. The increases in *a<sub>C</sub>* can be analyzed by MO calculations similar to those used for ion pair calculations.<sup>13,14</sup> The change required for the oxygen Coulomb parameters in order to take care of the effects of the first step solvation is 0.3-0.35 β for the free ion in DMF and all the ion pairs except for the lithium pair. The perturbation is slightly larger for the ion pairs with larger cations. This magnitude of perturbation is about the same as that produced by the sodium ion in the ion pair and similar to that found for alcohol solvated anthraquinone anions.<sup>14</sup>

**B. *a<sub>M</sub>* and *a<sub>C</sub>* for the Second Solvated Complex.** The increase of the <sup>13</sup>C splittings by solvation with the second alcohol is relatively small, being on the order of 1 G. This implies that the additional perturbation caused by the solvation is relatively weak compared with that by the first one. *a<sub>M</sub>* decreases largely upon second alcohol solvation. This indicates that the cations are further separated from the anion or the cation approaches more to the "in the plane" position upon the second step.

In the first step of solvation it was assumed that the solvation sphere of the cation is not much affected, but only the position of the cation changes. The second alcohol solvation seems to change the solvation sphere. Alcohols may solvate the cation and pull the cation more from the anion. If this is the case the electrostatic interaction between cation and anion is reduced by the second solvation making the increase of perturbation by the second solvation relatively small. This may be the reason for the relatively small changes of *a<sub>C</sub>* upon the second solvation.

(13) T. Takeshita and N. Hirota, *J. Amer. Chem. Soc.*, **93**, 6421 (1971).

(14) K. S. Chen and N. Hirota, *J. Amer. Chem. Soc.*, **94**, 5550 (1972).

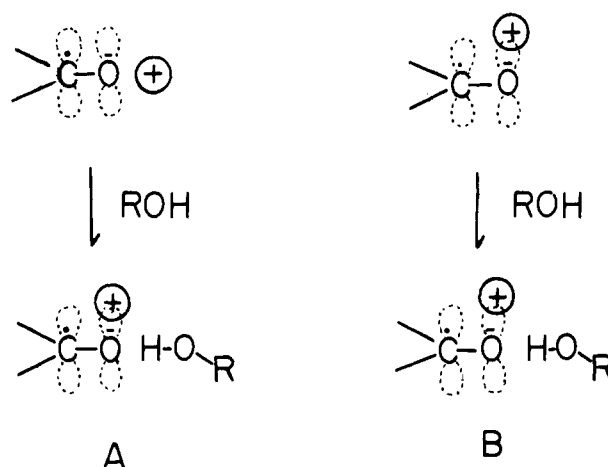


Figure 5. A suggested model of alcohol solvation for the ketyl ion pairs in the A and B forms.

In order to fit the alkali metal splittings of several systems, small negative values have to be assumed for *a<sub>M</sub>* for the second solvated species. This is reasonable if the position of the metal ion is close to the "in the plane" position in the second solvated complex. Such negative splittings have been observed commonly for the fluorenone ketyls in THF at very low temperatures.<sup>4</sup>

**C. *a<sub>M</sub>* and *a<sub>C</sub>* for the Third Solvated Complex.** *a<sub>C</sub>* of this complex was chosen to be smaller than those of the ion pairs in pure solvent. In view of the results obtained in the studies of DMF solvation to cation,<sup>4</sup> the *a<sub>M</sub>* were chosen to be larger than the values in pure THF. Although process II is important only in the Li pair, the minor contributions from this process were taken into consideration in other systems.

**D. Equilibrium Constants and General Trends of Solvation.** The equilibrium constants which best fit the curves were tabulated in Table I. Since reasonably good fits can be obtained by changing both *K* and *a*, it should be understood that these values of *K* are given in order to show the approximate values of the equilibrium constants. The numerical values of *K*<sub>1</sub> may be subject to uncertainties of ±20%. Other *K* values have more uncertainties. In spite of these uncertainties one can safely make several conclusions about the general trends of the solvation of ketyl ion pairs by alcohol. These are summarized below.

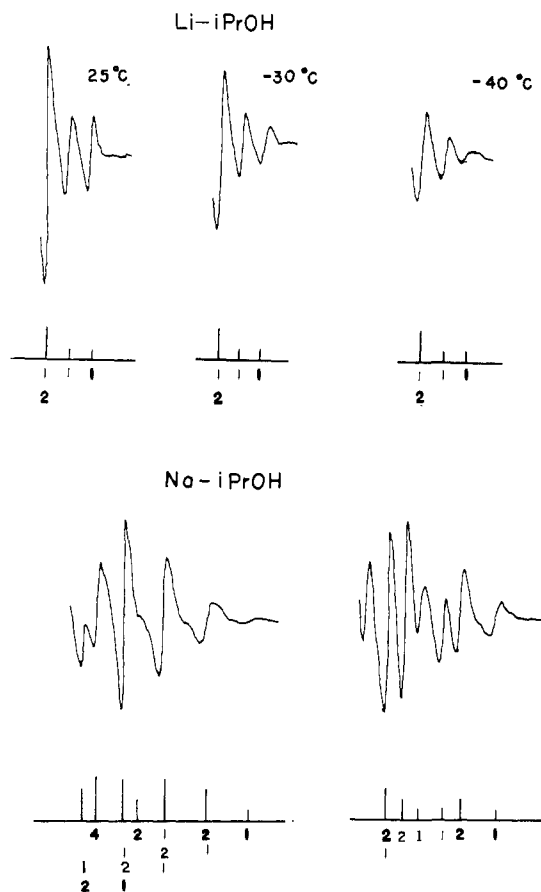


Figure 6. Solvation-induced  $M_z$ -dependent broadenings of lithium and sodium fluorenone ketyls in *i*-PrOH-THF mixtures. Top figure: Li in 2 mol % of *i*-PrOH in THF. Bottom figure: Na in 2 mol % of *i*-PrOH in THF (left at  $-70^\circ$  and right at  $-50^\circ$ ). The stick diagram indicates the intensity ratios predicted by assuming equal line widths for all lines. The number below the stick diagram indicates the relative intensities of each component. Numbers written by bold figures correspond to the relative intensities of the lines with  $M_z = 3/2$ . These lines are subject to more broadening.

- i.  $K_1$  and  $K_3$  become larger as the size of the cation increases.
- ii.  $K_2$  is larger than  $K_1$  only in the Li pair.
- iii. For the same metal ion  $K_1$  and  $K_3$  are larger for smaller alcohols.
- iv. For the same metal ion and alcohol  $K_1$  and  $K_3$  increase at lower temperatures.

Observations i and ii can be understood in the following way. First, a smaller cation has a more tightly bound solvation sphere which interferes with the solvation by alcohol. Second, the positive ion associated with the carbonyl oxygen tends to cancel the negative charge of oxygen, weakening the hydrogen-bond formation. This effect is particularly strong when the cation is small. In the ion pairs of small cations, cations occupy the "in the plane" position. This may also prevent more alcohol solvation. In the case of the Li pair, the solvation by alcohol to anion is so weakened that alcohol solvates cation more easily. Observation iii seems to indicate that the steric effect is significant in the solvation process. However, the observed sequence of the strength of solvation also follows the sequence of the polarity of the alcohol, and presumably both factors play an important role

in determining the equilibrium constants. We cannot decide which factor is more important at this point.

**5. Solvation of Alcohol in Other Ion Paired Radical Anions.** Although we did not make any detailed investigations of the solvation processes in other radical anions, a similar process of alcohol solvation was found in nitrobenzene anions and quinoxalines. In these systems, increases of the alkali metal splittings and the nitrogen splittings were observed upon addition of alcohol.

**6. The Line-Width Variations and the Dynamics of the Solvation Process.** The differences in hfs between the solvated and unsolvated species are usually quite large and the solvation processes produce modulations of isotropic hyperfine interactions large enough to cause line broadenings at low temperatures. Such broadenings were observed in the  $^{13}\text{C}$  splitting and the Na and Li splittings.

**A.  $^{13}\text{C}$  Splittings.** The differences in the hyperfine splittings between the solvated and the unsolvated species are of the order of 2–4 G. Therefore, the solvation-induced broadening of the  $^{13}\text{C}$  splittings is observable even at relatively high temperatures. This was clearly the case in sodium fluorenone in 2% *i*-PrOH solution. The intensity ratios of the  $^{13}\text{C}$  lines vs. the  $^{12}\text{C}$  lines were studied in pure THF and the 2% *i*-PrOH solution. The  $^{13}\text{C}$  lines in the 2% *i*-PrOH solution become much more broadened at relatively higher temperature compared with the case in pure THF.

**B. Alkali Metal Splittings.** Marked  $M_z$ -dependent line broadenings were observed in most Na and Li systems at lower temperatures. Here  $M_z$  is the magnetic quantum number of the alkali metal nuclei. Some examples are shown in Figure 6. It is clearly seen that the lines corresponding to  $M_z = \pm 3/2$  are much broader than those corresponding to  $M_z = \pm 1/2$ . In the case of the Li-BuOH system this broadening is observable even at room temperature.

**C. Solvation-Induced Line Broadening.** In the solvated complexes the location of the alkali metal ion and the alcohol may fluctuate rapidly. Assuming that the line broadening due to this fluctuation is smaller than the broadening caused by solvation and desolvation, one can make kinetic measurements of such processes. Since at least two solvation steps are taking place simultaneously, complete analysis of the line width is complex. However, when  $\chi$  is small in sodium fluorenone, the contribution of process II can be neglected compared with the contribution of process I. Under this condition, the solvation process is approximated by the two-jump process and the rate constant  $k_1$  can be estimated by the formula<sup>11</sup>

$$k_1 = 2.03 \times 10^7 \frac{P_u^2 P_s^2 (1 + K[\text{ROH}])(H_s - H_u)^2}{\delta H[\text{ROH}]} M^{-1} \text{sec}^{-1} \quad (4)$$

and  $k_{-1}$  is given by  $k_{-1} = k_1/K_1$ . Here  $\delta H$  is the broadening due to the solvation process.  $P_s$  and  $P_u$  are the fractions of the solvated and unsolvated species.  $H_s - H_u$  is the difference in the hyperfine frequencies between the solvated and unsolvated species.

When  $\chi$  is large process I is essentially completed. This is particularly so at low temperatures. However, the experiments show that there are still marked

$M_z$ -dependent line-width variations. The concentration dependence of the line broadening was studied in the case of sodium and lithium fluorenone. It was shown that  $\delta H$  measured at 2 and 10% of *i*-PrOH are very similar. From eq 4 the concentration dependence of  $\delta H$  is given by

$$\delta H \propto \frac{P_s^4}{K_1^2[\text{ROH}]^2} \left( K^2 + \frac{1}{[\text{ROH}]} \right) \quad (5)$$

If the first solvation process only is the cause of the broadening, the ratio of  $\delta H$  at 2 and 10% should be 6 to 1. Clearly this does not agree with the observation that  $\delta H$  at 2 and at 10% are almost the same. Therefore, it is concluded that the broadenings at 10% are primarily due to the second solvation processes.

The  $M_z$ -dependent line broadening in the case of Li is much more pronounced than the case of Na. Since  $H_s - H_u$  is slightly smaller for Li, the solvation rate for Li ketyls is much slower than the sodium ketyl. Li ketyl-*t*-BuOH-THF gives  $M_z$ -dependent line broadening even at room temperature. Therefore the solvation of *t*-BuOH is much slower than that of *i*-PrOH. Quite clearly the solvation rates are dependent on the nature of the metal ion and the type of alcohol. It appears that the rates are slower when the cation is smaller and the alcohol is more bulky.

#### D. Determination of the Rate Constants of the Solvation Process and the Lifetimes of the Solvated Complex.

In order to make an accurate determination of the solvation rate constants one has to know accurate values of the splittings of the solvated species and the equilibrium constants as well as  $\delta H$ . Since the solvation process is not a single step reaction, accurate determination of these quantities is very difficult. Also, the differences in the  $g$  values between the solvated and unsolvated species make the accurate estimates of  $H_u - H_s$  difficult. We made estimates of the rate constants in the case of the sodium fluorenone-*i*-PrOH system using the parameters which best fit the observed splittings vs. mole fraction of PrOH curves. Because of the relatively large uncertainties in  $a_C$ ,  $a_{Na}$ ,  $K$ , and  $\delta H$ , it should be realized that the obtained values of  $k_1$  and  $k_{-1}$  have large uncertainties (perhaps by a factor of 2). Nevertheless, these estimates give the approximate values for the rate constant for solvation and desolvation. The estimates of  $k_1$  were made from the broad-

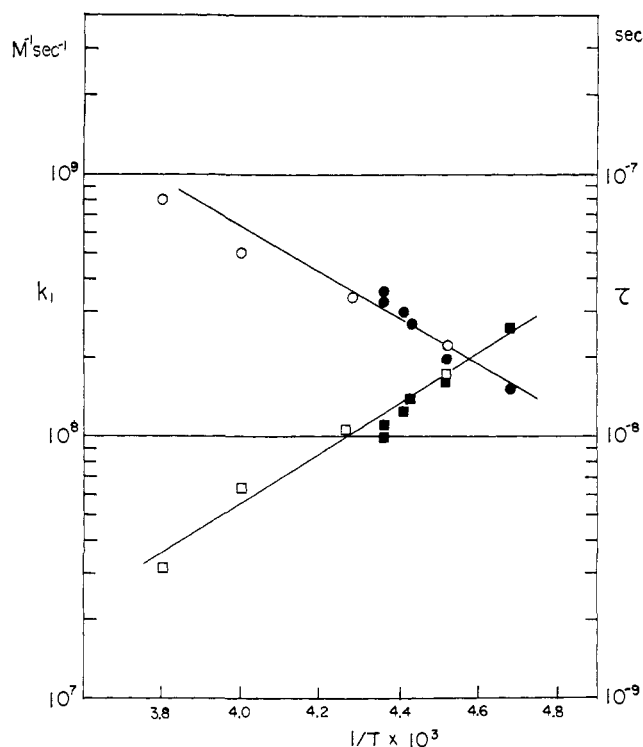


Figure 7. Plots of  $\log k_1$  and  $\log \tau$  vs.  $1/T$ :  $\square$  and  $\circ$  were determined from the broadenings of the  $^{13}\text{C}$  lines;  $\blacksquare$  and  $\bullet$  were determined from the broadenings of the sodium lines;  $\circ$  and  $\bullet$ ,  $k_1$ ;  $\square$  and  $\blacksquare$ ,  $\tau$ .

enings of the  $^{13}\text{C}$  lines and the Na lines. The values determined from the  $^{13}\text{C}$  lines and the Na lines are in good agreement as shown in Figure 7. In Figure 7 the estimated  $k_1$  and the lifetimes of the solvated complex  $\tau$  are given at different temperatures. The plots of  $k_1$  vs.  $1/T$  give the estimate of the activation energy to be  $\sim 4$  kcal/mol $^{-1}$  and  $k_1 \sim 10^9$   $M^{-1}$  sec $^{-1}$ , at  $0^\circ$ . The rate constant seems to be close to the diffusion-controlled rate constant.  $k_{-1}$  at  $0^\circ$  is  $5 \times 10^8$  sec $^{-1}$  or the lifetime of the solvated complex is  $\sim 2 \times 10^{-9}$  sec at  $0^\circ$ .

**Acknowledgment.** This work was supported by a grant from the National Science Foundation and a research fellowship from the A. P. Sloan Foundation to N. H. We gratefully acknowledge their support.